

# Characterization and Preferential Solvation of the Hexane/Hexan-1-ol/Methylbenzoate Ternary Solvent

S. Aparicio, R. Alcalde, J. M. Leal,\* and B. García

Universidad de Burgos, Departamento de Química, 09001 Burgos, Spain

Received: December 7, 2004; In Final Form: January 31, 2005

The thermophysical properties of the hexane/hexan-1-ol/methylbenzoate ternary system and its binary constituents were studied at 298.15 K over the whole composition range. The excess and mixing properties calculated from the experimental values combined with the mixture activity coefficients deduced from the UNIFAC group contribution method were used to calculate the integrals of the Kirkwood–Buff fluctuation theory for the ternary system and the binary constituents. Also the local composition and the excess or deficit number of molecules around a central molecule have been determined. The volumetric properties for the ternary system and its binary constituents were correlated and predicted successfully with several cubic equations of state combined with two simple mixing rules. The structural and intermolecular interactions of the mixtures were analyzed on the basis of the measured and derived properties.

## Introduction

This work contributes to an improved understanding of the thermophysical properties of binary and ternary mixtures containing aromatic esters.<sup>1</sup> Aromatic esters are known to exhibit a specific behavior due to self-aggregation. Although thermophysical properties of binary mixtures abound in the scientific literature, such data measured for benzoate-containing ternary systems have been rather scarcely investigated up to now.<sup>2–7</sup> Due to its aromatic electronic system and the hydrophobic and aprotic character, alkylbenzoates are frequently used in the industry as selective solvents.<sup>8</sup> Methylbenzoate is a polar ( $\mu = 1.94$  D), nonprotogenic selective solvent with important applications in the purification of solvents. Alkanes, however, are the simplest class of organic compounds, and the smaller alkanes play an important role as model molecules for the behavior of larger compounds.

To get both a deeper insight into the structure and intermolecular forces of systems involving aromatic esters and a set of reliable thermophysical data for chemical applications, a broad and systematic study of the properties of these systems is advisable. In this work, the densities, dynamic viscosities, and refractive indices of the hexane/hexan-1-ol/methylbenzoate ternary mixture are reported together with the hexane/hexan-1-ol, hexane/methylbenzoate, and hexan-1-ol/methylbenzoate binary constituents at 298.15 K and atmospheric pressure over the full composition range. In addition to the measured properties, the derived excess and mixing properties are reported as well. On the basis of the experimental results, interpretation of the intermolecular forces and evaluation of the preferential solvation of the molecules in the ternary system is feasible.<sup>9</sup> A valuable tool to study this phenomenon is the Kirkwood–Buff fluctuation theory of mixtures;<sup>10</sup> this model was revealed as a rigorous and general statistical thermodynamics model and has become a powerful tool to study mixed solvents behavior.<sup>11</sup> This theory links macroscopic thermodynamic properties with a microscopic structural description and can in principle be used

to predict a number of thermodynamic properties. However, after the work by Ben-Naim<sup>12</sup> the methodology was inverted, i.e., the Kirkwood–Buff integrals evaluated with the measured properties are used to draw reliable conclusions on the solution structure, since these integrals may provide information on both the local environment and the preferential solvation effect.

To properly determine the Kirkwood–Buff integrals, three properties are needed, partial molar volumes, isothermal compressibility coefficients, and activity coefficients. In this work, the partial molar volumes were evaluated from the experimental densities, the mixture compressibility coefficients were regarded as additive from those of the pure components, and the activity coefficients were calculated from the Dortmund UNIFAC group contribution model.<sup>13</sup> Data for ternary and multicomponent mixtures are still uncommon because of the time-consuming effort required to reach a proper set of accurate data; a useful approach consists of predicting the properties of multicomponent mixtures from the experimental data of the binary constituents, but this alternative route requires testing the reliability of such estimations and to assess whether the ternary interaction contributions should be taken into consideration.<sup>14</sup>

To reliably predict ternary properties, two routes can in principle be selected. On one hand, the ability of several symmetric and asymmetric semiempirical models to predict the excess and mixing properties derived from the experimental ones were studied.<sup>14</sup> On the other hand, the capability of the cubic equation of state by Soave (SRK)<sup>15</sup> and Peng–Robinson (PR)<sup>16</sup> using two simple mixing rules was applied to estimate the molar excess volumes of the ternary mixtures using binary interaction parameters only. The viscosity values of the ternary mixtures were also predicted using the predictive group contributions models by Wu<sup>17</sup> and GC–Unimod.<sup>18</sup>

## Experimental Section

**Materials.** The solvents *n*-hexane (99.5%), hexan-1-ol (99.9%), and methylbenzoate (MB, 99.9%), of the highest purity commercially available, were used without further purification. The purity was assessed by gas chromatography (GC) with a Perkin-

\* Author to whom correspondence should be addressed. E-mail: jmleal@ubu.es.

**TABLE 1:  $A_i$  Coefficients of Eq 5 and Standard Deviation,  $\sigma$ , for the  $x$  Hexane/(1 -  $x$ ) Hexan-1-ol Binary System at 298.15 K; Excess Molar Volume,  $V_m^E$  ( $\text{cm}^3 \text{mol}^{-1}$ ), Mixing Viscosity,  $\Delta_{\text{mix}}\eta$  (mPa s), and Mixing Refractive Index,  $\Delta_{\text{mix}}n_D$** 

property	$A_0$	$A_1$	$A_2$	$A_3$	$A_4$	$\sigma$
$V_m^E$	-0.6770	0.8380	0.0960	0.3741	0.9565	0.0016
$\Delta_{\text{mix}}\eta$	-6.000	2.881	-0.993	-0.305	1.143	0.010
$\Delta_{\text{mix}}n_D$	0.01015	-0.00875	-0.00560	-0.00415		0.00003

**TABLE 2:  $B_i$  Coefficients of Eq 6 and Standard Deviation,  $\sigma$ , for the  $x_1$  Hexane/ $x_2$  Hexan-1-ol/(1 -  $x_1$  -  $x_2$ ) MB Ternary System at 298.15 K; Excess Molar Volume,  $V_{m,\text{TER}}^E$  ( $\text{cm}^3 \text{mol}^{-1}$ ), Mixing Viscosity,  $\Delta_{\text{mix}}\eta_{\text{TER}}$  (mPa s), and Mixing Refractive Index,  $\Delta_{\text{mix}}n_{D,\text{TER}}$** 

property	$B_0$	$B_1$	$B_2$	$\sigma$
$V_{m,\text{TER}}^E$	1.5019	-2.5119	-3.4563	0.0360
$\Delta_{\text{mix}}\eta_{\text{TER}}$	-0.028	5.452	-1.441	0.031
$\Delta_{\text{mix}}n_{D,\text{TER}}$	0.20611	-0.22023	-0.22992	0.00072

Elmer 990 gas chromatograph, equipped with a Hewlett-Packard 3390A integrator, and also by comparing the densities, viscosities, and refractive indices with literature values (Supporting Information, Table S1, refs 19–30 contained therein). The pure liquids were degassed with ultrasound for several days before use and kept out of the light over Fluka Union Carbide 0.4 nm molecular sieves. The samples were prevented from preferential evaporation by syringing amounts, weighed to  $\Delta m = \pm 10^{-5}$  g with a Mettler AT 261 Delta Range balance, into suitably stoppered bottles. The mixtures were fully miscible over the whole composition range.

**Instruments and Procedures.** The molar excess volumes ( $\pm 10^{-4} \text{ cm}^3 \text{mol}^{-1}$ ) were deduced from the densities of the pure liquids and mixtures. The densities,  $\rho$ , were measured with a computer-controlled mechanical oscillator Anton Paar DMA 58 digital density meter (sample size  $0.7 \text{ cm}^3$ , accuracy  $\pm 3 \times 10^{-5} \text{ g cm}^{-3}$ , precision  $\pm 5 \times 10^{-6} \text{ g cm}^{-3}$ ) equipped with a Peltier element that ensures thermostatzation ( $\pm 0.01 \text{ K}$ ). Proper calibration was achieved at all working temperatures with deionized doubly distilled water (Milli-Q, Millipore) and *n*-nonane (Fluka, 99.2% GC) as reference liquids.

Dynamic viscosities,  $\eta$ , were measured with an automated AMV 200 Anton Paar microviscometer, which requires only a very small sample volume. Viscosity measurements were based on the rolling ball measuring principle. A gold-covered steel ball was introduced into an inclined, sample-filled, thermostated ( $\pm 0.005 \text{ K}$ ) glass capillary, and the rolling time  $t$  ( $\pm 0.01 \text{ s}$ ) needed for the ball to roll a fixed distance between two magnetic sensors was converted into viscosity readings ( $\pm 0.005 \text{ mPa s}$ ). The calibration constants at every inclination angle and working temperature were evaluated as a function of the standard liquid and the density of the ball ( $7.874 \text{ g cm}^{-3}$ ) in the form

$$k(\alpha) = \eta_{\text{stand}}/(\rho_{\text{ball}} - \rho_{\text{stand}})t \quad (1)$$

where  $k(\alpha)$  is the calibration constant at each inclination angle,  $\eta_{\text{stand}}$  is the dynamic viscosity of the standard liquid,  $\rho_{\text{ball}}$  is for the density of the ball, and  $\rho_{\text{stand}}$  is for that of the standard liquid. A computerized Anton Paar SPV sample changer was used, the injection of the sample being automatically achieved with a peristaltic pump.

The refractive indices,  $n_D$  ( $\pm 5 \times 10^{-5}$ ), were measured using the sodium line of an automatic Leica AR600 refractometer. Small sample volumes were put on a prism equipped with a tight-fitting lid that preserves the sample from preferential evaporation; the thermostatic time of the samples was small,

and the temperature (Julabo F32MV thermostat,  $\pm 0.01 \text{ K}$ ) was read at the prism surface. The  $n_D$  values were taken every 2 min as an average of 150 readings.

## Results

Experimental densities, dynamic viscosities, and refractive indices for the *n*-hexane/hexan-1-ol binary constituent (Table S2) and for the *n*-hexane/hexan-1-ol/MB ternary system (Table S3) at 298.15 K over the full composition range are reported as Supporting Information; the properties of the other two binary constituents were reported previously.<sup>1a,b</sup> The extent to which liquid mixtures deviate from ideal behavior is best reflected by the derived thermodynamic excess functions instead of the raw experimental data.<sup>31</sup> In this work, the excess molar volumes,  $V_m^E$ , were calculated from the measured density data according to eq 2

$$V_m^E = \frac{M}{\rho} - \sum_{i=1}^N \left( x_i \frac{M_i}{\rho_i} \right) \quad (2)$$

Likewise, for the nonthermodynamic properties dynamic viscosity and refractive index, the so-called mixing properties were calculated for the mixing viscosity,  $\Delta_{\text{mix}}\eta$ , and mixing refractive index,  $\Delta_{\text{mix}}n_D$ , defined according to eqs 3 and 4, respectively

$$\Delta_{\text{mix}}\eta = \eta - \sum_{i=1}^N x_i \eta_i \quad (3)$$

$$\Delta_{\text{mix}}n_D = n_D - \sum_{i=1}^N x_i n_{D,i} \quad (4)$$

The excess and mixing properties of the binary systems are attributed to the different shapes and sizes of the components, to the reorientation of the molecules in the mixture, and to the molecular interactions; these are termed  $Y^E$  in eq 5 and were correlated with composition using the Redlich–Kister polynomials<sup>32</sup>

$$Y^E = x(1-x) \sum_{i=1}^r A_i (2x-1)^i \quad (5)$$

the coefficients being deduced by a least-squares procedure using the Marquardt algorithm, and the proper number of coefficients,  $r$ , being determined by a  $F$ -test. Table 1 lists the Redlich–Kister coefficients for the *n*-hexane/hexan-1-ol binary constituent; those for *n*-hexane/MB and hexan-1-ol/MB were reported previously.<sup>1a,b</sup> Figure 1 plots the experimental and correlated excess and mixing properties for the three binary constituents at 298.15 K. With aid of the Redlich–Kister coefficients evaluated with eq 5 for the binary constituents, the excess and mixing properties for the  $x_1$  hexane/ $x_2$  hexan-1-ol/(1 -  $x_1$  -  $x_2$ ) MB ternary system,  $Y_{\text{TER}}^E$ , were correlated with composition using the Cibulka equation<sup>33</sup>

$$Y_{\text{TER}}^E = Y_{\text{BIN}}^E + x_1 x_2 (1 - x_1 - x_2) (B_0 + B_1 x_1 + B_2 x_2) \quad (6)$$

where  $Y_{\text{BIN}}^E$  represents the sum extended to the three binary constituents, eq 7

$$Y_{\text{BIN}}^E = Y_{12}^E + Y_{13}^E + Y_{23}^E \quad (7)$$

the  $Y_{ij}^E$  binary contributions being evaluated for each property from eq 5 and the  $B_i$  parameters determined by least-squares

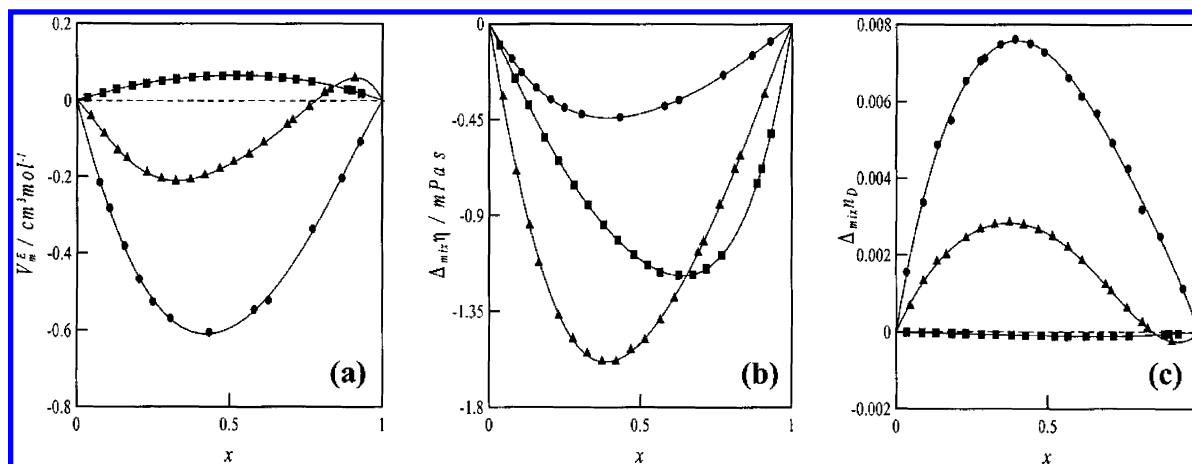


**Figure 1.** (a) Excess molar volume,  $V_m^E$ , (b) mixing viscosity,  $\Delta_{\text{mix}}\eta$ , and (c) mixing refractive index,  $\Delta_{\text{mix}}n_D$ , at 298.15 K for the  $x$  hexane/(1 -  $x$ ) MB<sup>1a</sup> (●),  $x$  hexan-1-ol/(1 -  $x$ ) MB<sup>1b</sup> (■), and  $x$  hexane/(1 -  $x$ ) hexan-1-ol (▲) binary systems.

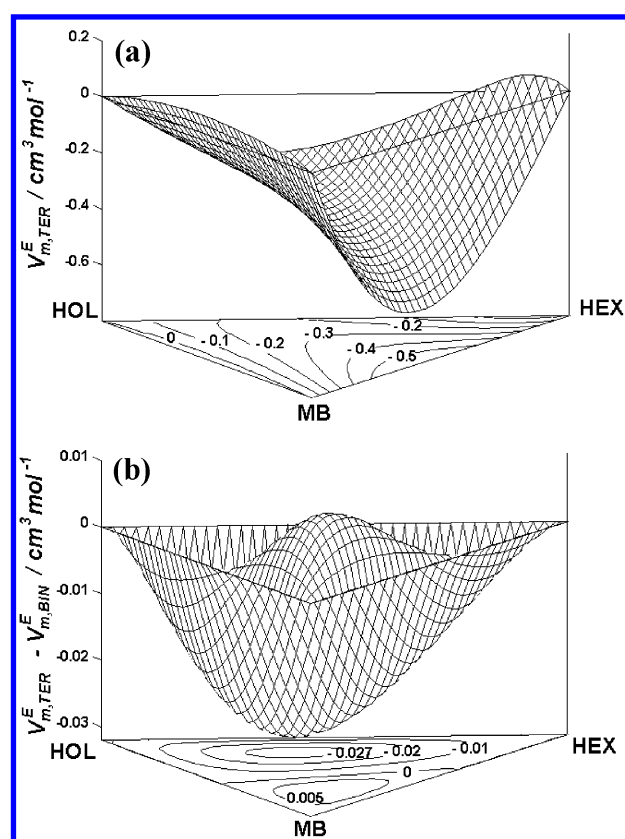


**Figure 2.** (a) Excess molar volume,  $V_{m,\text{TER}}^E$ , and (b) ternary contribution of excess molar volume,  $V_{m,\text{TER}}^E - V_{m,\text{BIN}}^E$ , at 298.15 K for the  $x_1$  hexane/ $x_2$  hexan-1-ol/(1 -  $x_1 - x_2$ ) MB ternary system.

fitting (Table 2). Valuable information on the ternary interactions can be deduced from the so-called “ternary contributions” ( $Y_{\text{TER}}^E - Y_{\text{BIN}}^E$ ) calculated with eqs 6 and 7, which represent the difference between the measured value for the ternary property and that evaluated using the data for the binary constituents. The excess and mixing properties and the ternary contributions for the ternary system are plotted in Figures 2–4; the maxima and/or minima of the ternary contributions are listed in Table 3. Likewise, the correlating Cibulka functions combined with the coefficients for the molar excess volume (Table 2) have enabled the partial molar excess volumes of the ternary components,  $\bar{V}_{m,\text{TER}i}^E$ , to be calculated using the intercept method<sup>1a,b</sup> (Figure 5).

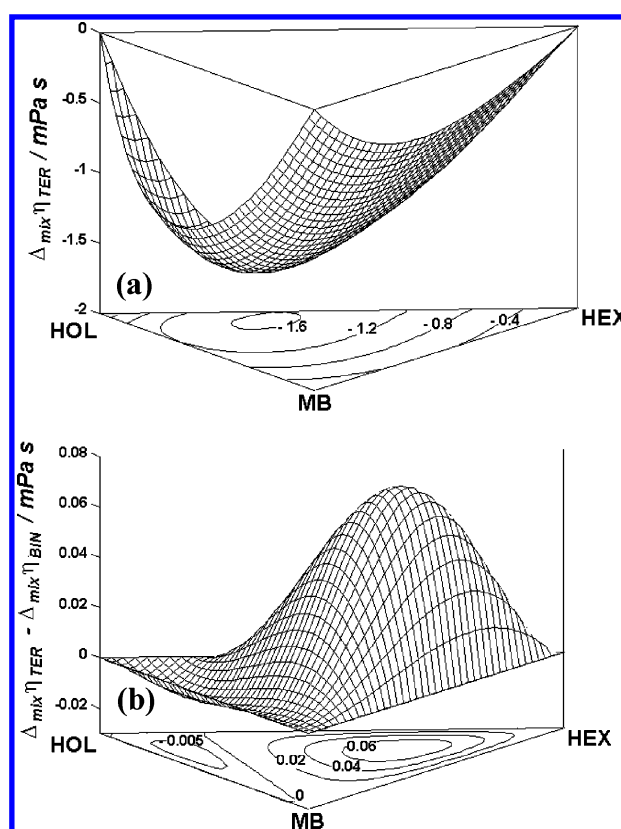


**Figure 3.** (a) Mixing viscosity,  $\Delta_{\text{mix}}\eta_{\text{TER}}$ , and (b) ternary contribution of mixing viscosity,  $\Delta_{\text{mix}}\eta_{\text{TER}} - \Delta_{\text{mix}}\eta_{\text{BIN}}$ , at 298.15 K for the  $x_1$  hexane/ $x_2$  hexan-1-ol/(1 -  $x_1 - x_2$ ) MB ternary system.

## Discussion

The structural effects and intermolecular interactions in multicomponent mixtures can be inferred from the amount and the sign of the excess and mixing properties. The properties calculated for pure hexan-1-ol indicate strong self-association by hydrogen bonding; for mixed hexan-1-ol, however, such an association effect depends on the cosolvent nature. Recent studies on hexan-1-ol/hexane binary mixtures point to alcohol self-aggregation in *n*-hexane, this effect giving rise to 4–5 predominantly cyclic-membered clusters.<sup>34,35</sup> The hexane/MB binary system is prone to dispersion forces;<sup>1a</sup> these lead to the disruption of the dipolar ordering in pure MB and further packing caused by the similar lengths of the linear alkane and the planar MB. However, for hexan-1-ol/MB, the properties

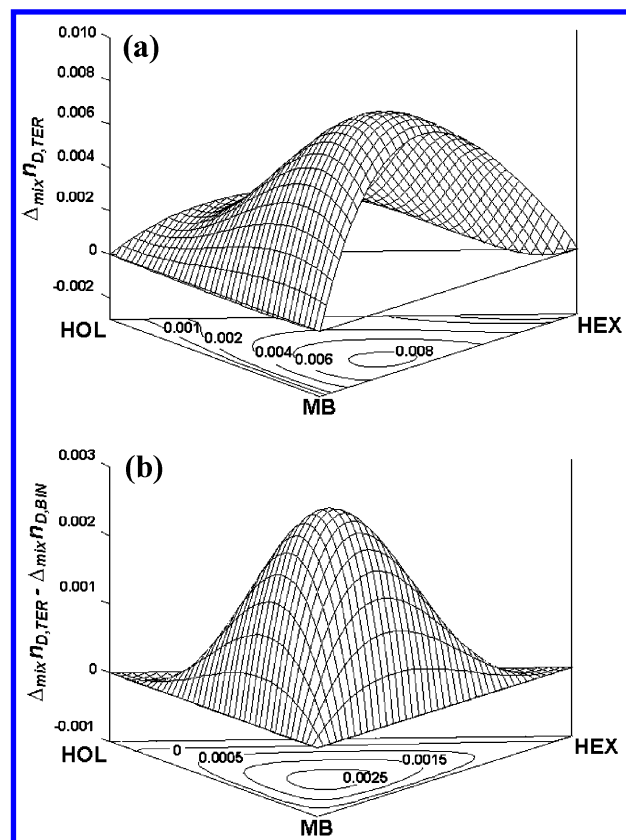


**Figure 4.** (a) Mixing refractive index,  $\Delta_{\text{mix}}\eta_{D,\text{TER}}$ , and (b) ternary contribution of mixing refractive index,  $\Delta_{\text{mix}}\eta_{D,\text{TER}} - \Delta_{\text{mix}}\eta_{D,\text{BIN}}$ , at 298.15 K for the  $x_1$  hexane/ $x_2$  hexan-1-ol/(1 -  $x_1$  -  $x_2$ ) MB ternary system.

indicate breaking of the alcohol hydrogen bonds upon mixing with MB;<sup>1b</sup> although certain dipolar alcohol–ester interactions are feasible, these are not sufficient to balance the disruption of the hydrogen-bond ordering and the efficient package, since the size effects are unimportant. Comparison of the excess and mixing properties for the three binary constituents (Figure 1) confirm the above conclusions. In contrast to the positive values for hexan-1-ol/MB, the negative hexane/MB excess molar volumes denote both the effective hexane packing in the MB structure<sup>1a</sup> and the disruption of the alcohol hydrogen-bonding structure upon mixing with the ester. An intermediate situation occurs in the hexane/hexan-1-ol binary system, which exhibits an S-shaped curve with positive values in the alkane-rich zones, and the alcohol hydrogen-bond structure remains in the hexane-rich zones; although formation of ring structures by the hexan-1-ol clusters is feasible,<sup>35</sup> the alcohol is minority in the binary mixture and positive molar excess volumes result.

The negative mixing viscosities deduced for the three binary constituents reveal the prevalence of dispersion forces;<sup>36</sup> these were highest for hexane/hexan-1-ol and decreased from hexan-1-ol/MB to hexane/MB. Although certain alcohol hydrogen-bonding structure remains in hexane/hexan-1-ol, the alcohol

dilution by the nonpolar hexane causes a decrease in the mixture viscosity. For hexan-1-ol/MB, the disruption of the alcohol hydrogen-bonding structure by the polar MB is the predominant effect (consistent with the positive molar excess volumes), which is not fully balanced by possible dipole–dipole alcohol associations. For hexane/MB, the steric hindrance due to the packing effect appears as the most relevant factor, the negative mixing viscosities denoting the prevalence of binary dispersion forces. The behavior of the mixing refractive indices also is consistent with these conclusions; systems with negative molar excess volumes lead to positive mixing refractive indices, for contractive mixing processes, the number of dipoles per unit volume increases,<sup>37</sup> and thus the mixing refractive indices increase (Figure 1, parts a and c).

The properties of the hexane/hexan-1-ol/MB ternary system (Figures 2–4) show only moderate ternary effects. The molar excess volumes were mainly negative over nearly the full composition range (Figure 2a); only in the hexane-rich areas or near the hexan-1-ol binary mixtures these were positive; therefore the above-mentioned effects for the three binary constituents remain in the ternary system. The ternary contribution to the excess molar volume was primarily small and negative (Figure 2b), with a minimum in the MB-poor zones (Table 3), which represents some 11% of the value at that composition, and a maximum in MB-rich zones, which represents some 3% of the value at that composition. Thus, the ternary effects, mainly steric, are noticeably weak due to (i) the very different shapes of the three components that produce a certain expansion when MB is prevalent, (ii) the alcohol hydrogen-bonding disruption produced by the ester (positive ternary contribution), and (iii) certain ternary contraction (negative ternary contribution) when MB is not prevailing caused by the more similar shapes of alkane and alcohol and the remaining alcohol hydrogen-bonding structure.

The mixing viscosities, negative throughout (Figure 3a) with a minimum close to the hexan-1-ol/hexane minimum (Table 3), indicate that dispersion forces are the main intermolecular interactions in the mixture; the ternary contribution, mainly positive (Figure 3b), displayed a maximum in the hexane-rich region, which represents 7.7% of the value at that composition; also this contribution manifests a short negative hexanol-rich region, with a minimum that represents 0.53% of the value at that composition. The modest amount of the ternary contributions indicate small ternary effects on this property; the predominantly positive mixing viscosities coincide with the maximum in the hexane-rich regions because the hydrogen-bonding disruption effect of MB on hexan-1-ol becomes diluted by hexane, with the result of a slightly positive contribution to mixing viscosities (positive ternary contribution). On the contrary, when hexane is in the minority, such a dilution does not occur (negative ternary contribution).

The positive ternary mixing refractive indices deduced, with a maximum near the hexane/MB binary constituent (Figure 4a), are consistent with the negative excess molar volumes (Figure

**TABLE 3: Coordinates for the Maxima and Minima of the Ternary Contributions to Excess Molar Volume,  $V_{\text{m,TER}}^E - V_{\text{m,BIN}}^E$  ( $\text{cm}^3 \text{mol}^{-1}$ ), Mixing Viscosity,  $\Delta_{\text{mix}}\eta_{\text{TER}} - \Delta_{\text{mix}}\eta_{\text{BIN}}$  (mPa s), and Mixing Refractive Index,  $\Delta_{\text{mix}}\eta_{D,\text{TER}} - \Delta_{\text{mix}}\eta_{D,\text{BIN}}$  for the  $x_1$  Hexane/ $x_2$  Hexan-1-ol/(1 -  $x_1$  -  $x_2$ ) MB Ternary System at 298.15 K**

	$V_{\text{m,TER}}^E - V_{\text{m,BIN}}^E$		$\Delta_{\text{mix}}\eta_{\text{TER}} - \Delta_{\text{mix}}\eta_{\text{BIN}}$		$\Delta_{\text{mix}}\eta_{D,\text{TER}} - \Delta_{\text{mix}}\eta_{D,\text{BIN}}$	
	position	amount	position	amount	position	amount
maximum	$x_1 = 0.1750$ $x_2 = 0.1367$	0.0097	$x_1 = 0.5321$ $x_2 = 0.2186$	0.074	$x_1 = 0.2414$ $x_2 = 0.2358$	0.00292
minimum	$x_1 = 0.3334$ $x_2 = 0.4844$	−0.0297	$x_1 = 0.0754$ $x_2 = 0.6716$	−0.008	$x_1 = 0.3774$ $x_2 = 0.5805$	−0.00011



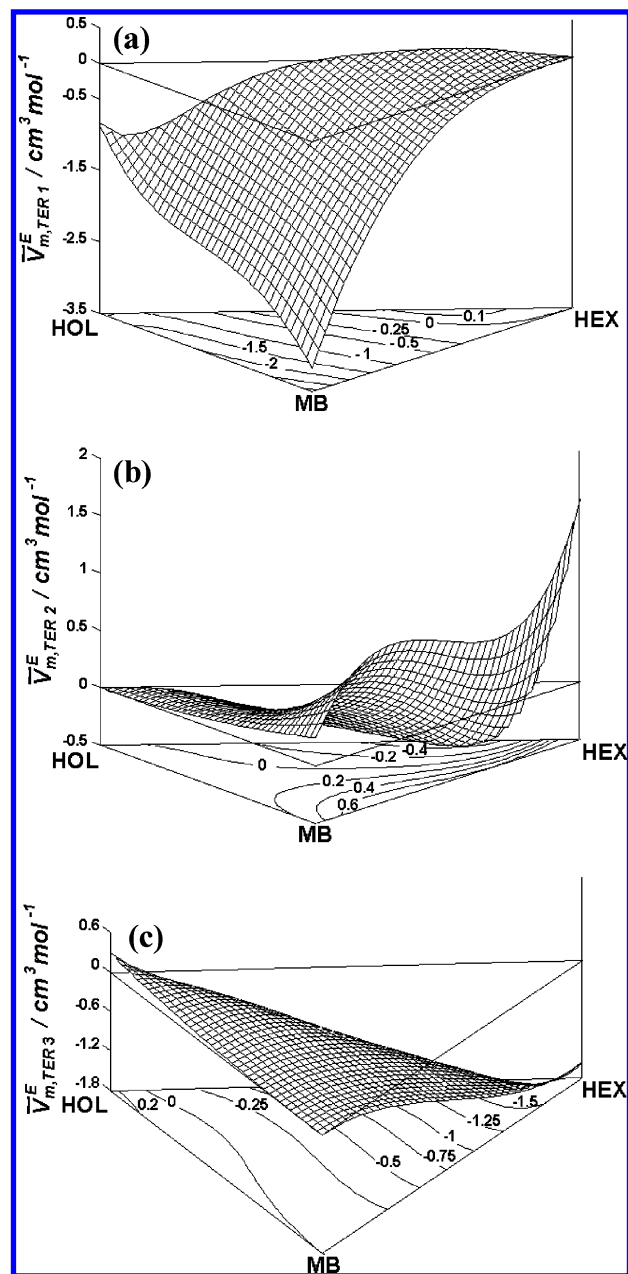


**Figure 5.** (a) Excess partial molar volume of *n*-hexane,  $\bar{V}_{m,TER1}^E$ , (b) hexan-1-ol,  $\bar{V}_{m,TER2}^E$ , and (c) MB,  $\bar{V}_{m,TER3}^E$ , at 298.15 K for the  $x_1$  hexane/ $x_2$  hexan-1-ol/(1 -  $x_1$  -  $x_2$ ) MB ternary system.

2a) and can be explained by the dipole concentration in this region; the ternary contributions were mainly positive (Figure 4b) with a maximum that represents 38.3% of the property. Although the mixing contraction increases the dipole density, this effect is not followed by stronger dipole–dipole interactions, as confirmed by the negative mixing viscosities (Figure 3a).

Finally, the behavior of the partial molar excess volumes of the three ternary components is rather complex (Figure 5). Some authors have indicated that large and positive  $\bar{V}_{m,TERi}^E$  values denote an ordering rupture, whereas negative values denote specific interactions between components;<sup>38</sup> therefore, the positive values for hexan-1-ol in the MB-rich zones (Figure 5b) indicate hydrogen-bonding disruption by the ester, and negative values in hexane-rich zones indicate that the alcohol structure partly remains in the nonpolar alkane. The very positive partial molar excess volumes for hexan-1-ol when hexane is almost pure indicate that although the hydrogen bonds could remain

these are diluted in the alkane, which prevents them from forming alcohol clusters. The  $\bar{V}_{m,TERi}^E$  hexane values were primarily negative (Figure 5a), with a minimum in MB-rich zones, this feature caused by the alkane-packing effect in the planar ester structure; also the negative values in hexan-1-ol-rich zones could be explained by the similar shape of both molecules. The  $\bar{V}_{m,TERi}^E$  MB values were positive only in zones where MB or hexan-1-ol are prevailing (Figure 5c), confirming the MB disruption effect on the alcohol structure whereas, due to the packing effect,  $\bar{V}_{m,TERi}^E$  values were negative in zones where the alkane prevails.

**Kirkwood–Buff Theory.** Further conclusions into the structure of this system can be drawn using the Kirkwood–Buff theory, often called fluctuation theory, which is a fundamental tool for the investigation and understanding of solution structure. The preferential solvation effect is always present and affects the thermodynamic properties of mixtures; preferential solvation arises when the local mole fraction of the components in the solvation microsphere differs from those of the bulk composition. This model provides new relationships between thermodynamic quantities and molecular distribution functions and enables us to draw microscopic features of mixtures from measurable thermodynamic quantities. After the pioneering work by Ben-Naim et al.<sup>12a</sup> enabled us to apply the model to binary mixtures, the theory has been widely used to interpret the properties of liquid mixtures and the solvent structure. The link between microscopic and macroscopic thermodynamic properties is provided by the so-called Kirkwood–Buffs integrals,  $G_{ij}$ , which are computed according to eq 8

$$G_{ij} = \int_0^\infty (g_{ij} - 1) 4\pi r^2 dr \quad (8)$$

where  $g_{ij}$  represents the radial distribution function of species  $i$  around the central molecule  $j$  and  $r$  is the distance between the centers of the two molecules.

Matteoli et al.<sup>39</sup> pointed out that if the Kirkwood–Buff integrals of mixtures are examined to get an insight into interactions and local mixture compositions, then a suitable reference level must be established. The symmetrical ideal system can then be regarded as a suitable reference level, i.e., to obtain reliable information on the mixture structure the  $G_{ij}$  values for this reference level should be subtracted from the  $G_{ij}$  mixture values. The expressions for the  $G_{ij}$  values used in this work for the binary constituents and the ternary mixture were obtained from Ruckenstein et al.<sup>40</sup> according to the above criteria. Another important parameter in the application of the Kirkwood–Buff theory is the excess number of molecules around a central one,  $n_{ij}$ . This property can be calculated from the  $G_{ij}$  values according to eq 9

$$n_{ij} = c_i(G_{ij} - G_{ij}^{\text{IDEAL}}) \quad (9)$$

**Source of Data.** Evaluation of the  $G_{ij}$  integrals requires use of three macroscopic thermodynamic properties, isothermal compressibilities, activity coefficients, and partial molar volumes. Partial molar volumes for the ternary mixture and its binary constituents were evaluated from the experimental excess molar volumes according to the intercept method (Figure 5). The contribution of the isothermal compressibilities of the mixtures to  $G_{ij}$  is almost negligible;<sup>40</sup> therefore they were regarded as ideal and determined from the literature values for the pure compounds.<sup>20</sup> To properly determine the partial derivatives of the chemical potential, the activity coefficients and their concentration dependence are needed; unfortunately

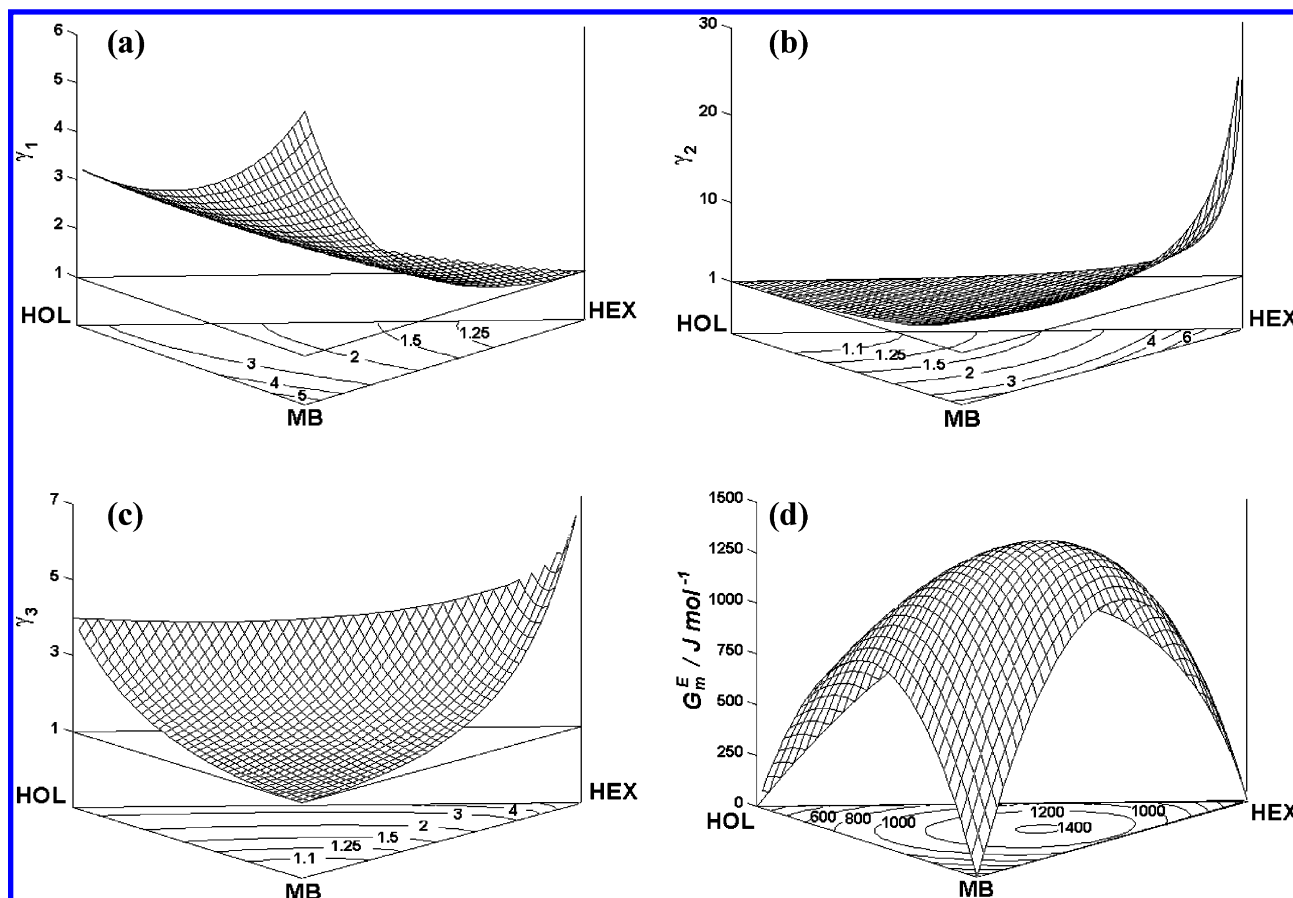


**Figure 6.** Activity coefficients of (a) *n*-hexane,  $\gamma_1$ , (b) hexan-1-ol,  $\gamma_2$ , and (c) MB,  $\gamma_3$ , and (d) excess molar Gibbs energies,  $G_m^E$ , at 298.15 K for the  $x_1$  hexane/ $x_2$  hexan-1-ol/(1 -  $x_1$  -  $x_2$ ) MB ternary system calculated using the Dortmund UNIFAC group contribution model and the parameters by Gmehling et al.<sup>13</sup>

these are not experimentally available; therefore they were evaluated using the Dortmund UNIFAC group contribution method.<sup>13</sup> The broad data basis used in this work to obtain the group parameters enables the model to afford reliable and accurate results.

**Results and Analysis.** Figure 6 plots the activity coefficients calculated together with the excess free energies. The behavior of the activity coefficients was similar to that of the partial molar excess volumes (Figure 5) and supports the conclusions drawn from the properties analyzed. It is remarkable that the high hexan-1-ol activity coefficients in hexane-rich regions are concordant with the slightly positive molar excess volumes (Figure 2a) and the high and positive partial molar excess volumes (Figure 5b). Positive and large excess free energies are consistent with the conclusions drawn with the above properties.

The  $G_{ij}$  integrals were calculated at 298.15 K for the three binary constituents and the ternary mixture. In fact, the ternary mixture was treated as a pseudo-binary mixture, i.e., a ternary mixture with constant mole fraction for one of the three ternary components and variable composition for the other two. Two pseudo-binary mixtures were in principle considered,  $x'$  hexan-1-ol/(1 -  $x'$ ) MB, with hexane mole fraction constant to 0.1 and  $x'$  hexane/(1 -  $x'$ ) MB, with hexan-1-ol mole fraction constant to 0.1. Figure 7 plots the data for the binary mixtures. The slightly positive  $G_{\text{HEX-HEX}}$  values (Figure 7a) in contrast to the strongly negative  $G_{\text{HOL-HOL}}$  values should be noted; this result illustrates that hexane is preferentially solvated by hexane; for hexan-1-ol, however, the hydrogen-bonding structure remains only in the high dilution region limit, where  $G_{\text{HOL-HOL}}$  becomes positive. The lack of affinity between the hexane and

hexan-1-ol molecules is clearly reflected by the negative  $G_{\text{HEX-HOL}}$  values. The positive  $n_{\text{HEX-HEX}}$  values (Figure 7b) and the negative  $n_{\text{HOL-HOL}}$  values confirm that hexane is preferentially solvated by hexane. However, despite the low alkane-alcohol affinity (Figure 7a), hexan-1-ol is preferentially solvated by hexane; therefore hydrogen bonding between alcohol molecules is feasible only in the highly diluted zone (Figure 7d). This feature is consistent with the slightly positive molar excess volumes in the very diluted region (Figure 1a). In conclusion, this system displays a complicated preferential solvation behavior.

The behavior of the properties for the hexane/MB binary constituent is shown in Figure 8. The Kirkwood-Buff integrals deduced for these systems were very high, positive for  $G_{ii}$  and negative for  $G_{ij}$  (Figure 8a) with well-defined maxima and minima, respectively. The lack of affinity between hexane and MB, revealed by the negative  $G_{\text{HEX-MB}}$  values, is also confirmed by the large and positive  $n_{ii}$  and large but negative  $n_{ij}$  values (Figure 8, parts b and c). This means that the hexane molecules are primarily surrounded by hexane molecules, while the MB molecules are preferentially solvated by MB molecules; the high (either positive or negative) integrals indicate a high solvation sphere radius. Although the negative molar excess volumes denote an efficient packing, the above findings can be explained assuming that the difference in shape of both molecules (linear hexane, planar MB) favors the preferential solvation between like molecules.

The Kirkwood-Buff analysis of the hexan-1-ol/MB binary constituent is shown in Figure 9. The  $G_{ii}$  values were positive, but not too high, whereas  $G_{ij}$  values were negative, but also not too high, i.e., once again the solvation sphere of each

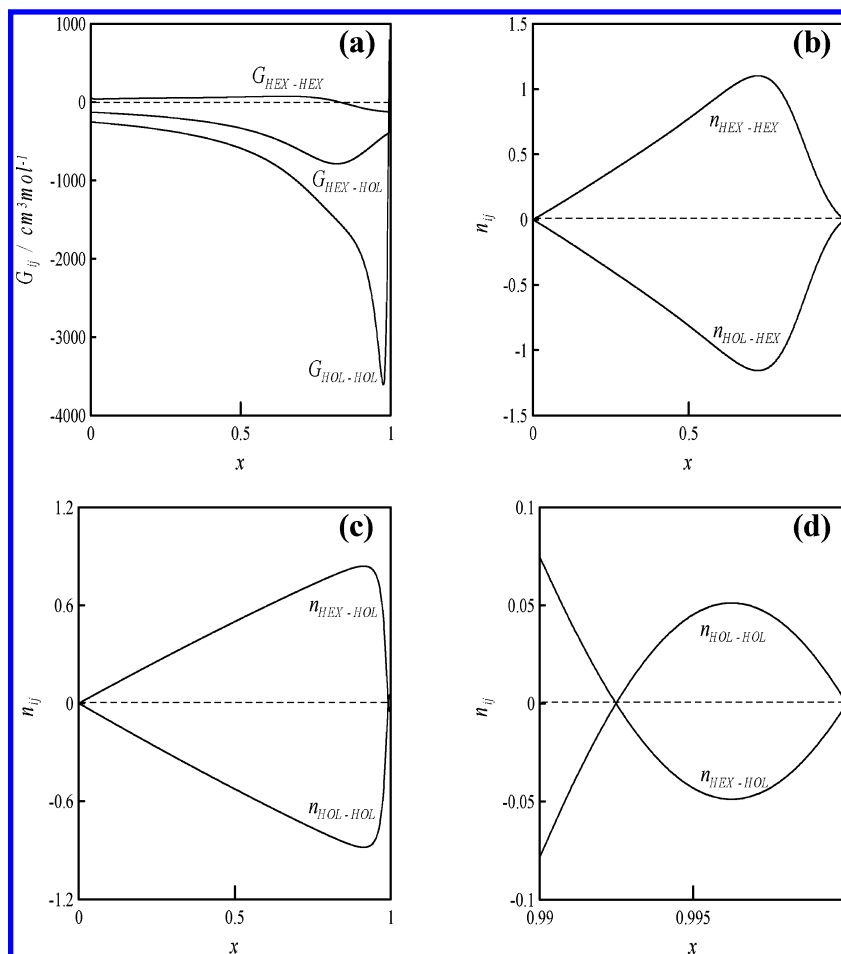


**Figure 7.** (a) Kirkwood–Buff integrals  $G_{ij}$ , (b) excess or deficiency of molecules around a central hexane molecule, (c) around a central hexan-1-ol molecule, and (d) magnification of Figure 6c in the hexan-1-ol highly dilute region, for the  $x$  hexane/(1 -  $x$ ) hexan-1-ol binary systems at 298.15 K.

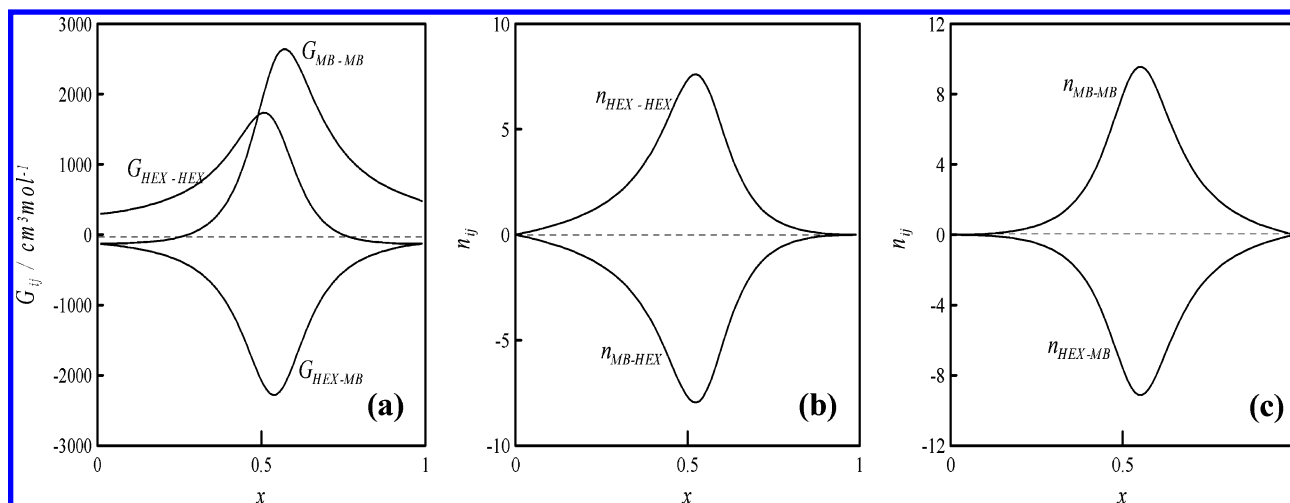


**Figure 8.** (a) Kirkwood–Buff integrals  $G_{ij}$ , (b) excess or deficiency of molecules around a central hexane molecule, and (c) around a central MB molecule in the hexane/MB binary systems at 298.15 K.

molecule is mainly formed by like molecules (Figure 9, parts b and c). Although the integral values and the excess number of molecules around a central one are not high and the solvation radius is small, the resulting intermolecular interactions between alcohols are not too efficient, because the positive excess molar volume prevails (Figure 1a).

Application of the model to the ternary system was performed according to the pseudo-binary approach. Figure 10 shows the results for  $x'$  hexan-1-ol/(1 -  $x'$ ) MB with a constant hexane

mole fraction of 0.1. Figure 10a shows the excess or deficiency of molecules around a central hexane molecule; the behavior of this property is complex and points to like–like preferential solvation (positive  $n_{\text{HEX-HEX}}$ ). Only at low MB concentration hexane becomes solvated by the alcohol; in any event the alkane is not solvated by MB, and the alkane solvation sphere is small (Figure 10a). For hexan-1-ol, Figure 10b shows preferential like–like solvation. Comparison of Figures 10b and 9b indicates that solvation of hexan-1-ol is unaffected by hexane addition

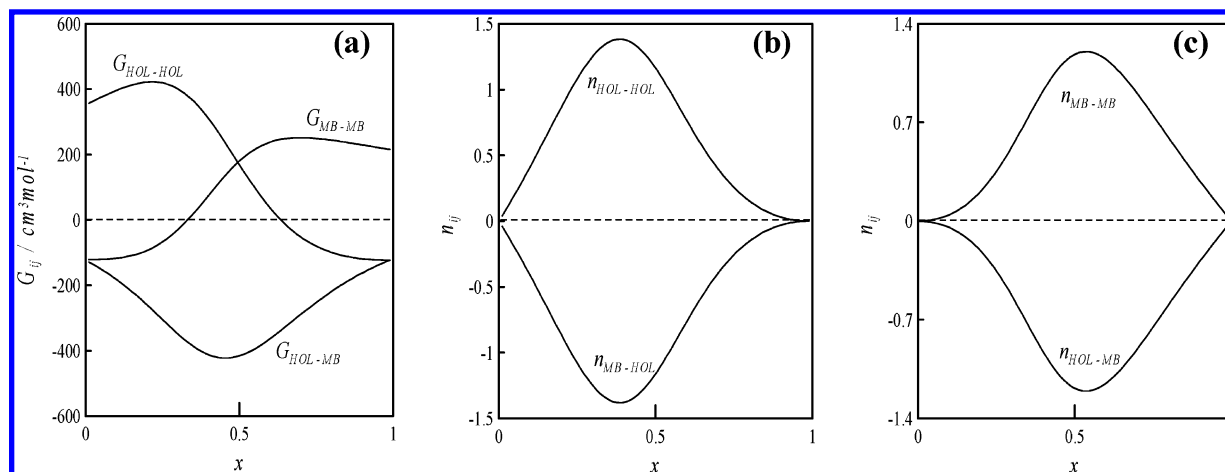


**Figure 9.** (a) Kirkwood-Buff integrals  $G_{ij}$ , (b) excess or deficiency of molecules around a central hexan-1-ol molecule, and (c) around a central MB molecule in the hexan-1-ol/MB binary systems at 298.15 K.

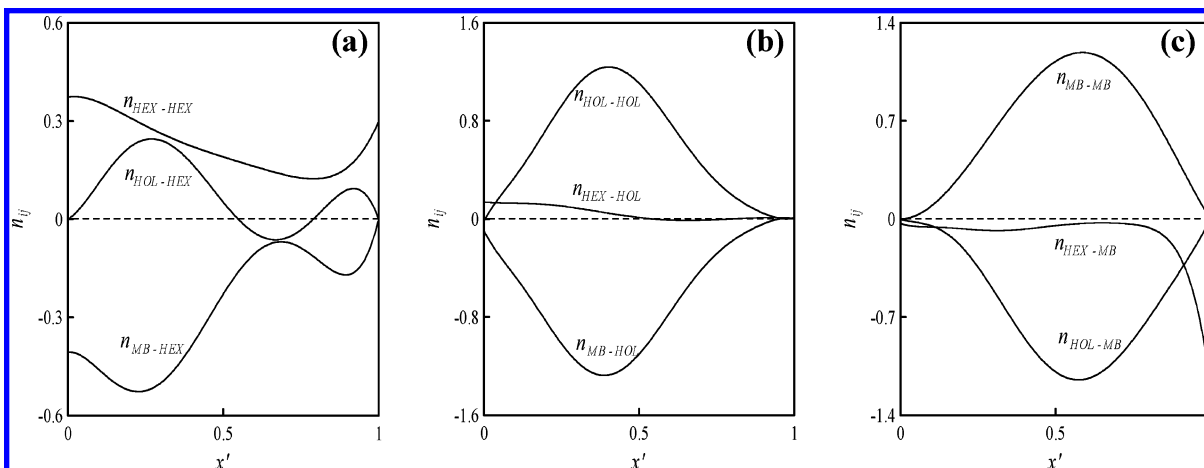


**Figure 10.** Excess or deficiency of molecules (a) around a central hexane molecule, (b) around a central hexan-1-ol molecule, and (c) around a central MB molecule, in the pseudo-binary system hexane/hexan-1-ol/MB with  $x_{\text{hexane}} = 0.1$  at 298.15 K.  $x' = x_{1-\text{hexanol}}/(x_{1-\text{hexanol}} + x_{\text{MB}})$ .

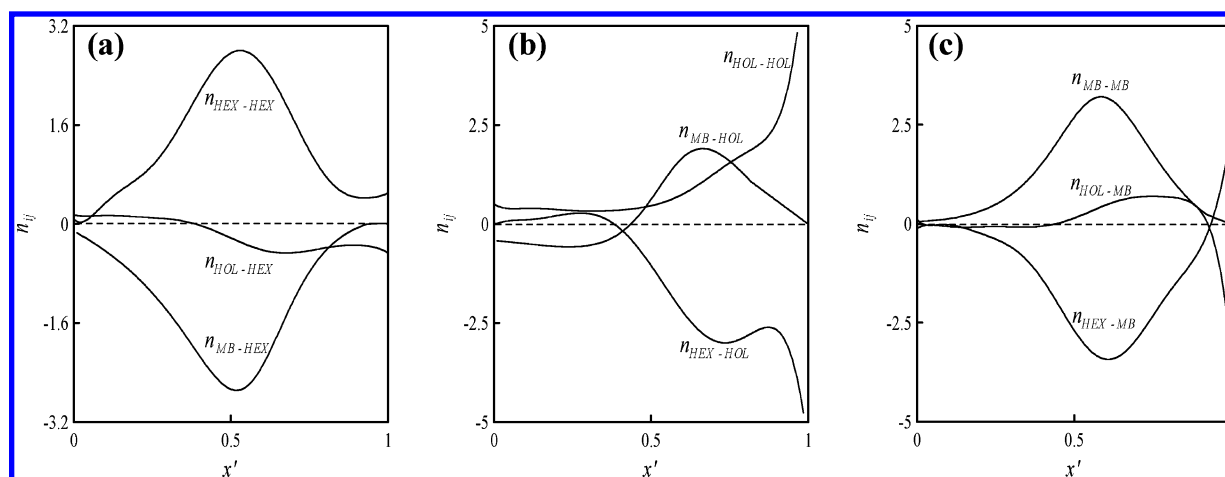


**Figure 11.** Excess or deficiency of molecules (a) around a central *n*-hexane molecule, (b) around a central hexan-1-ol molecule, and (c) around a central MB molecule, in the pseudo-binary system hexane/hexan-1-ol/MB with  $x_{\text{hexan-1-ol}} = 0.1$  at 298.15 K.  $x' = x_{\text{hexane}}/(x_{\text{hexane}} + x_{\text{MB}})$ .

to the hexan-1-ol/MB mixture; instead the positive  $n_{\text{HEX-HOL}}$  values reveal only a soft hexane solvation in the MB diluted regions; the solvation sphere, though small, was greater than that for hexane (Figures 10, parts a and b). MB suffers preferentially like-like solvation (Figure 10c); the negative  $n_{\text{HOL-MB}}$  values indicate absence of hexan-1-ol molecules in the MB solvation sphere, whereas hexane molecules appear to be excluded only in the high MB concentration zones. Comparison of Figures 10c and 9c indicate a weak effect on the

MB solvation sphere by addition of hexane to the hexan-1-ol/MB mixture.

Figure 11 plots the results for the  $x'$  hexane/(1 -  $x'$ ) MB pseudo-binary mixture with a constant hexan-1-ol mole fraction of 0.1. The excess or deficiency of molecules around a central hexane molecule is shown in Figure 11a, around a central hexan-1-ol molecule in Figure 11b, and around a central MB molecule in Figure 11c. Hexane is preferentially solvated by like molecules; comparison of Figures 11a and 8b reveals that,



**TABLE 4: Standard Deviations,  $\sigma$ , for the Predictions Obtained with Semiempirical Models for the  $x_1$  Hexane/ $x_2$  Hexan-1-ol/(1 –  $x_1$  –  $x_2$ ) MB Ternary System at 298.15 K**

model	$\sigma(V_{m,TER}^E)$ (cm <sup>3</sup> mol <sup>-1</sup> )			$\sigma(\Delta_{mix}\eta_{TER})$ (mPa s)			$\sigma(\Delta_{mix}n_{D,TER})$		
Jacob–Fitzner	0.0420			0.044			0.00140		
Köhler	0.0426			0.062			0.00141		
Colinet	0.0422			0.059			0.00141		
Tsao–Smith	0.0420 <sup>a</sup>	0.0756 <sup>b</sup>	0.0420 <sup>c</sup>	0.295 <sup>a</sup>	0.034 <sup>b</sup>	0.298 <sup>c</sup>	0.00110 <sup>a</sup>	0.00110 <sup>b</sup>	0.00132 <sup>c</sup>
Toop	0.0451 <sup>a</sup>	0.0528 <sup>b</sup>	0.0498 <sup>c</sup>	0.127 <sup>a</sup>	0.092 <sup>b</sup>	0.097 <sup>c</sup>	0.00110 <sup>a</sup>	0.00152 <sup>b</sup>	0.00162 <sup>c</sup>
Scatchard	0.0451 <sup>a</sup>	0.0511 <sup>b</sup>	0.0504 <sup>c</sup>	0.113 <sup>a</sup>	0.093 <sup>b</sup>	0.091 <sup>c</sup>	0.00111 <sup>a</sup>	0.00161 <sup>b</sup>	0.00161 <sup>c</sup>

<sup>a</sup> For asymmetric equations, the component 1 is hexane. <sup>b</sup> For asymmetric equations, the component 1 is hexan-1-ol. <sup>c</sup> For asymmetric equations, the component 1 is MB.

**TABLE 5:  $k_{12}$  and  $m_{12}$  Parameters and Standard Deviations,  $\sigma$ , Obtained in the Application of Soave (SRK) and Peng–Robinson (PR) Cubic EOS with the  $R_1$  and  $R_2$  Mixing Rules for the Correlation (Binary Systems) and Prediction (Ternary System) of Excess Molar Volumes (cm<sup>3</sup> mol<sup>-1</sup>) at 298.15 K<sup>a</sup>**

mixture	SRK					PR				
	$R_1$		$R_2$			$R_1$		$R_2$		
	$k_{12}$	$\sigma$	$k_{12}$	$m_{12}$	$\sigma$	$k_{12}$	$\sigma$	$k_{12}$	$m_{12}$	$\sigma$
hexane/hexan-1-ol	0.0994	0.0626	0.0662	–0.0072	0.0099	0.0939	0.0375	0.0641	–0.0065	0.0160
hexane/MB	0.0944	0.0379	0.0805	–0.0040	0.0189	0.0842	0.0177	0.0849	–0.0017	0.0176
hexan-1-ol/MB	0.0008	0.0007	0.0007	–0.0067	0.0007	0.0023	0.0008	0.0013	–0.0068	0.0007
hexane/hexan-1-ol/MB		0.0541			0.0447		0.0563			0.0442

<sup>a</sup> Parameters for hexane/MB are from ref 1a, and those for hexan-1-ol/MB are from ref 1b.

although addition of hexan-1-ol to the hexane/MB mixture diminishes the hexane solvation sphere, hexane like–like solvation prevails, and a soft solvation of hexan-1-ol occurs at low MB concentration. Figure 11c denotes a complex behavior for hexan-1-ol, with preferential like solvation, and certain solvation by MB at intermediate concentrations. The MB solvation is preferentially produced by MB molecules (Figure 11c), although a certain solvation by hexan-1-ol appears that decreases when the alkane concentration increases. Figures 11c and 8c reveal that the MB solvation sphere decreases on addition of hexan-1-ol to the hexane/MB mixture, but this does not affect the sphere composition, which mainly consists of MB molecules.

It can then be concluded from the Kirkwood–Buff analysis that the very different shape and size of the three components, hexane, hexan-1-ol, and MB, lead to solvation spheres of like–like molecules, the size of which decreases upon addition of a third component to the binary mixtures. Hexan-1-ol is able to form hydrogen bonds only in the dilute regions when mixed with hexane, whereas these forces are noticeably weakened or even destroyed in MB mixtures and in the ternary mixture because the shape of the molecules makes contact between molecules difficult.

**Modeling of Thermophysical Properties. Semiempirical Models.** Although modern instrumentation enables us to obtain accurate thermophysical measurements for liquids, the determination of such properties in multicomponent mixtures at different temperatures and pressures and over the full composition range is both expensive and time-consuming.<sup>14</sup> A survey of the literature available shows that such data for ternary solvents are very scarce compared with binary solvents. So far, an objective of solution thermodynamics has been to develop reliable equations to predict properties of multicomponent mixtures from those of the binary constituents. The predictive ability of such equations is not general and often leads to worse predictions for systems where ternary effects are important; therefore to check their applicability, these models should be tested for different types of mixtures.

The above conclusions indicate that the hexane/hexan-1-ol/MB ternary system does not manifest pronounced ternary interactions, and thus the predictive models should produce good results. In this section, some semiempirical predictive equations

widely used are analyzed. These models are classified as asymmetric, if they are dependent on the arbitrary numbering of the mixture components, or symmetric. The symmetric models by Jacob–Fitzner,<sup>41</sup> Köhler,<sup>42</sup> and Colinet,<sup>43</sup> together with the asymmetric models by Tsao–Smith,<sup>44</sup> Toop,<sup>45</sup> and Scatchard<sup>46</sup> were tested, and the results of the prediction for  $V_{m,TER}^E$ ,  $\Delta_{mix}\eta_{TER}$ , and  $\Delta_{mix}n_{D,TER}$  are reported in Table 4. The three symmetric models gave good predictions for the three properties. To obtain lowest deviations with asymmetric models, numbering as 1 the common component of the two binary constituents with greater deviations from ideality is warmly recommended;<sup>47</sup> therefore this component should be hexane for excess molar volume and mixing refractive index and hexan-1-ol for mixing viscosity (Figure 1). This criterion leads to lower deviations for the three asymmetric models tested (Table 4). In any event, the predictions obtained with symmetric models are comparable to those afforded by the asymmetric models, even though the best predictions were obtained with the Tsao model. As a rule, absence of strong ternary interactions yields low deviations with any of the checked models.

**Cubic Equations of State.** The excess molar volumes and related properties are important tools in the calculations for process design and also for theoretical purposes; therefore, accurate predictions of these properties are required. The interest in theoretical and semiempirical work based on various equations of state (EOS) for the prediction of molar excess volumes of mixtures has increased in recent years.<sup>48</sup> The correlation and/or prediction of molar excess volumes relies on a careful choice of the selected EOS combined with a suitable mixing rule. Several authors have used the cubic EOS by Soave (SRK)<sup>15</sup> and Peng–Robinson (PR)<sup>16</sup> to determine volumetric properties of multicomponent mixtures and obtained good results even with mixtures of polar solvents. In this work, the following cubic EOS were applied

$$P = \frac{nRT}{V - nb} - \frac{n^2a}{(V + \delta_1 nb)(V + \delta_2 nb)} \quad (10)$$

with  $\delta_1 = 1$  and  $\delta_2 = 0$  for SRK and  $\delta_1 = 1 + \sqrt{2}$  and  $\delta_2 = 1 - \sqrt{2}$  for PR,  $n$  being the mole number in the mixture.

Application of this equation to multicomponent mixtures requires calculation of the copressure,  $a$ , and covolume,  $b$ , parameters evaluated from those of the pure components using the so-called mixing rules. The two simple mixing rules described by eqs 11 and 12 were used. The classical van der

$$a = \sum_{i=1}^r \sum_{j=1}^r x_i x_j (1 - k_{ij})(a_i a_j)^{0.5} \quad (11)$$

$$b = \sum_{i=1}^r \sum_{j=1}^r x_i x_j (1 - m_{ij})(b_i b_j)^{0.5} \quad (12)$$

Waals mixing rule for copressure factor, combined with the nonclassical mixing rule for the covolume factor, has been used successfully in highly nonideal systems, leading to accurate correlations and low deviations over wide pressure and temperature ranges;<sup>49</sup> therefore these rules were preferred instead of others with a deeper theoretical basis but whose complexity is not accompanied by better correlations. For the first mixing rule ( $R_1$ ), the  $k_{ij}$  parameters were fitted introducing the experimental  $V_m^E$  data and yielded  $m_{ij} = 0$ . For the second mixing rule ( $R_2$ ), the  $m_{ij}$  and  $k_{ij}$  parameters were also fitted. The fitting parameters were derived using the Marquardt algorithm combined with the Newton–Raphson method used to solve the equation of state; further details on the fitting procedure are given elsewhere.<sup>1a–c</sup>

Only binary interaction parameters are considered in the application of cubic EOS together with mixing rules eqs 11 and 12. Therefore, these models are correlative for the binary constituents, but they are predictive for the ternary system when using the parameters obtained from the binary constituents. Table 5 lists the results for the systems investigated. Low deviations are obtained in the correlation of molar excess volumes for the three binary constituents; both equations of state produce similar results when applied with the same mixing rule. The two-parameter mixing rule gave better correlations than the one-parameter, but in general the two rules provided good results. The predictive ability of these equations and mixing rules is rather good, including the one-parameter mixing rule. Thus, cubic EOS can be applied for the correlation of excess molar volumes in ester-containing binary mixtures, and hence the parameters obtained may afford highly qualified predictions in multicomponent mixtures.

**Predictive Semiempirical Viscosity Models.** Due to the pivotal role played by liquid viscosities in the design of industrial processes, the development of reliable theoretical models for the prediction of this property in binary and multicomponent solvents is a very important objective. The models by Wu<sup>17</sup> and Cao (GC-UNIMOD)<sup>18</sup> were applied on the basis of the UNIFAC group contribution concept, the group parameters required being obtained from Hansen et al.<sup>50</sup> The predictions obtained with both models for the hexane/hexan-1-ol/MB ternary system were not accurate enough, with a Wu standard deviation of 0.286 and GC-UNIMOD of 0.782; therefore, application of this model for the prediction of the dynamic viscosities in the ternary system investigated is not advisable, and the aforementioned strong intermolecular forces make it advisable to use more complex models to yield accurate predictions.

**Acknowledgment.** Financial support by Junta de Castilla y León, project BU10/03, and the Ministerio de Ciencia y Tecnología, Spain, project PPQ2002-02150, is gratefully acknowledged.

**Supporting Information Available:** Densities, dynamic viscosities and refractive indices of pure solvents,  $x$  *n*-hexane/(1 −  $x$ ) hexan-1-ol binary mixtures, and  $x_1$  *n*-hexane/ $x_2$  hexan-1-ol/(1 −  $x_1$  −  $x_2$ ) MB ternary mixture. This material is available free of charge via the Internet at <http://pubs.acs.com>.

## Nomenclature

- $x_i$  = mole fraction of the  $i$  component
- $\rho, \rho_i$  = density of the mixture and of the  $i$  component
- $\eta, \eta_i$  = dynamic viscosity of the mixture and of the  $i$  component
- $n_D, n_{D,i}$  = refractive index of the mixture and of the  $i$  component
- $M, M_i$  = molar mass of the mixture and of the  $i$  component
- $V_m^E, V_{m,TER}^E$  = excess molar volume of binary and ternary systems
- $\Delta_{mix}\eta, \Delta_{mix}\eta_{TER}$  = mixing viscosity of binary and ternary systems
- $\Delta_{mix}n_D, \Delta_{mix}n_{D,TER}$  = mixing refractive index of a binary and ternary system
- $\bar{V}_{m,TERi}^E$  = partial excess molar volumes of the  $i$  component of a ternary system
- $Y^E, Y_{TER}^E$  = symbol for a binary and ternary excess or mixing property
- $Y_{BIN}^E$  = binary contribution to a ternary excess or mixing property in eqs 6 and 7
- $A_i$  = Redlich–Kister correlating coefficients in eq 5
- $B_i$  = Cibulka correlating coefficients in eq 6
- $G_{ij}$  = Kirkwood–Buff integrals
- $n_{ij}$  = excess or deficiency number of molecules around a central one according to the Kirkwood–Buff theory
- $x'$  = mole fraction in a pseudobinary mixture
- $P$  = pressure
- $T$  = absolute temperature
- $R$  = universal gas constant
- $a$  = mixture copressure parameter in eq 10
- $b$  = mixture covolume parameter in eq 10
- $a_i$  = copressure parameter of  $i$ th component in eq 11
- $b_i$  = energetic parameter of  $i$ th component in eq 12
- $\delta_1$  = parameter in eq 10
- $\delta_2$  = parameter in eq 10
- $k_{ij}$  = parameter in eq 11
- $m_{ij}$  = parameter in eq 12
- $R_1$  = mixing rule 1 for eqs 11 and 12
- $R_2$  = mixing rule 2 for eqs 11 and 12
- HEX = hexane
- HOL = hexan-1-ol
- MB = methylbenzoate

## Errors

- $x_i = \pm 10^{-4}$
- $\rho = \pm 10^{-5} \text{ g cm}^{-3}$
- $\eta = \pm 10^{-3} \text{ mPa s}$
- $n_D = \pm 10^{-5}$
- $V_m^E = \pm 10^{-4} \text{ cm}^3 \text{ mol}^{-1}$
- $\Delta_{mix}\eta = \pm 10^{-3} \text{ mPa s}$
- $\Delta n_D = \pm 4 \times 10^{-5}$
- $\bar{V}_i^E = \pm 10^{-3} \text{ cm}^3 \text{ mol}^{-1}$

## References and Notes

- (1) (a) García, B.; Alcalde, R.; Aparicio, S.; Leal, J. M. *Ind. Eng. Chem. Res.* **2002**, *41*, 4399. (b) García, B.; Alcalde, R.; Aparicio, S.; Leal, J. M. *Phys. Chem. Chem. Phys.* **2002**, *4*, 5833. (c) García, B.; Alcalde, R.;

- Aparicio, S.; Leal, J. M. *J. Phys. Chem. B* **2003**, *107*, 13478. (d) García, B.; Miranda, M. J.; Leal, J. M.; Matos, J. S. *Thermochim. Acta* **1991**, *186*, 285.
- (2) Tsierekzos, N. G.; Kellarakis, A. E.; Molinou, I. E. *J. Chem. Eng. Data* **2000**, *45*, 776.
- (3) Semeniuk, B.; Wilczura-Wachnick, H. *Fluid Phase Equilib.* **1998**, *152*, 337.
- (4) Ortega, J.; Postigo, M. A. *Fluid Phase Equilib.* **1995**, *108*, 121.
- (5) (a) García, B.; Ortega, J. C. *J. Chem. Eng. Data* **1988**, *33*, 200. (b) García, B.; Ortega, J. C. *Thermochim. Acta* **1987**, *117*, 219.
- (6) Aminabhavi, T. M.; Phayde, H. T. S.; Khinnavar, R. S.; Gopalakrishna, B. *J. Chem. Eng. Data* **1994**, *39*, 251.
- (7) Dusart, O.; Piekarski, C.; Piekarski, S.; Viallard, A. *J. Chem. Phys.* **1976**, *78*, 837.
- (8) Grolrier, J. P. E.; Ballet, D.; Viallard, A. *J. Chem. Thermodyn.* **1974**, *6*, 895.
- (9) Zielkiewicz, J. *Phys. Chem. Chem. Phys.* **2000**, *2*, 2925.
- (10) Kirkwood, J. G.; Buff, F. P. *J. Chem. Phys.* **1951**, *19*, 774.
- (11) *Fluctuation Theory of Mixtures*; Matteoli, E., Mansoori, G. A., Eds.; Taylor and Francis: New York, 1992; p 372.
- (12) (a) Ben-Naim, A. *J. Chem. Phys.* **1977**, *67*, 4884. (b) Ben-Naim, A. *Statistical Thermodynamics for Chemists and Biochemists*; Plenum Press: New York, 1992; p 372.
- (13) Gmehling, J.; Li, J.; Schiller, M. *Ind. Eng. Chem. Res.* **1993**, *32*, 178.
- (14) Acree, W. E. *Thermodynamic Properties of Nonelectrolyte Solutions*; Academic Press: Orlando, FL, 1984; p 62.
- (15) Soave, G. *Chem. Eng. Sci.* **1972**, *27*, 1197.
- (16) Peng, Y.; Robinson, D. B. *Ind. Eng. Chem. Fundam.* **1976**, *15*, 59.
- (17) Wu, D. T. *Fluid Phase Equilib.* **1986**, *30*, 149.
- (18) Cao, W.; Knudsen, A.; Fredenslund, A.; Rasmussen, P. *Ind. Eng. Chem. Res.* **1993**, *32*, 2088.
- (19) Aminabhavi, T. M.; Raikar, S. K. *Collect. Czech. Chem. Commun.* **1993**, *58*, 1761.
- (20) Riddick, J. A.; Bunger, W. B.; Sakano, T. K. *Organic Solvents: Physical Methods of Purification*; John Wiley: New York, 1986.
- (21) Matilla, A. D.; Tardajos, G.; Junquera, E.; Aicart, E. *J. Sol. Chem.* **1991**, *20*, 805.
- (22) Ortega, J.; Legido, J. L. *Fluid Phase Equilib.* **1993**, *86*, 251.
- (23) Iglesias, T. P.; Legido, J. L.; Romaní, L.; Andrade, M. I. P. *Phys. Chem. Liq.* **1993**, *25*, 135.
- (24) Ambrose, D.; Tsonopoulos, C. *J. Chem. Eng. Data* **1995**, *40*, 531.
- (25) Dymond, J. H.; Oye, H. A. *J. Phys. Chem. Ref. Data* **1994**, *23*, 41.
- (26) Aralaguppi, M. I.; Jaddar, C. V.; Aminabhavi, T. M. *J. Chem. Eng. Data* **1999**, *44*, 435.
- (27) Liew, K. Y.; Seng, C. E.; Ng, B. H. *J. Sol. Chem.* **1993**, *22*, 1033.
- (28) Decominges, B. E.; Piñeiro, M. M.; Mosteiro, L.; Iglesias, T. P.; Legido, J. L.; Andrade, M. I. P. *J. Chem. Eng. Data* **2001**, *46*, 1206.
- (29) Jiménez, E.; Casas, H.; Segade, L.; Franjo, C. *J. Chem. Eng. Data* **2000**, *45*, 862.
- (30) Aminabhavi, T. M.; Aralaguppi, M. I.; Harogoppad, S. B.; Balundgi, R. M. *J. Chem. Eng. Data* **1993**, *38*, 31.
- (31) Rowlinson, J. S.; Swinton, F. L. *Liquids and Liquid Mixtures*; Butterworth: Boston, 1982; p 132.
- (32) Redlich, O.; Kister, A. T. *Ind. Eng. Chem.* **1948**, *40*, 345–348.
- (33) Cibulka, I. *Collect. Czech. Chem. Commun.* **1982**, *47*, 1414.
- (34) Gupta, R. B.; Brinkley, R. L. *AIChE. J.* **1998**, *44*, 207.
- (35) Stubbs, J. M.; Chen, B.; Potoff, J. J.; Siepmann, J. I. *Fluid Phase Equilib.* **2001**, *183–184*, 301.
- (36) Fort, R.; Moore, W. R. *Trans. Faraday Soc.* **1966**, *62*, 1112.
- (37) Iglesias, T. P.; Legido, J. L.; Pereira, S. M.; de Cominges, B. *J. Chem. Thermodyn.* **2000**, *32*, 923.
- (38) Domínguez, M.; Gascón, I.; Valén, A.; Royo, F. M.; Urieta, J. S. *J. Chem. Thermodyn.* **2000**, *32*, 1551.
- (39) Matteoli, E. *J. Phys. Chem. B* **1997**, *101*, 9800.
- (40) Ruckenstein, E.; Shulgin, I. *Fluid Phase Equilib.* **2001**, *180*, 281.
- (41) Jacob, K. T.; Fitzner, K. *Thermochim. Acta* **1977**, *18*, 197.
- (42) Köhler, F. *Monatsh. Chem.* **1960**, *91*, 738.
- (43) Colinet, C. Ph.D. Thesis. University of Grenoble, France, 1967.
- (44) Tsao, C. C.; Smith, J. M. *Chem. Eng. Prog. Symp. Ser.* **1953**, *49*, 107.
- (45) Toop, G. W. *Trans. TMS-AIME* **1965**, *223*, 850.
- (46) Scatchard, G.; Ticknor, L. B.; Goates, J. R.; McCartney, E. R. *J. Am. Chem. Soc.* **1952**, *74*, 3721.
- (47) Pando, C.; Renuncio, J. R.; Calzón, J. A. G.; Christensen, J. J.; Izatt, R. M. *J. Sol. Chem.* **1987**, *16*, 503.
- (48) (a) Iglesias, M.; Piñeiro, M. M.; Marino, G.; Orge, B.; Domínguez, M.; Tojo, J. *Fluid Phase Equilib.* **1999**, *154*, 123. (b) Serbanovic, S. P.; Djordjevic, B.; Grozdanic, D. *Fluid Phase Equilib.* **1990**, *57*, 47. (c) Adachi, Y.; Sugie, H. *J. Chem. Eng. Jap.* **1988**, *21*, 57.
- (49) Laugier, S.; Richon, D. *J. Chem. Eng. Data* **1997**, *42*, 155.
- (50) Hansen, H. K.; Rasmussen, P.; Fredenslund, A. *Ind. Eng. Chem. Res.* **1991**, *30*, 2352.